Published in final edited form as:
Cancer Res. 2007 June 15; 67(12): 5965–5975. doi:10.1158/0008-5472.CAN-06-3168.

Genetic Ablation of the Amplified-in-Breast Cancer-1 (AIB1) Inhibits Spontaneous Prostate Cancer Progression in Mice

Arthur C.-K. Chung[1,3], **Suoling Zhou**[1], **Lan Liao**[1], **Jean Ching-Yi Tien**[1], **Norman M. Greenberg**[2], and **Jianming Xu**[1,*]

[1] Department of Molecular and Cellular Biology, Baylor College of Medicine, Houston, Texas 77030

[2] Fred Hutchinson Cancer Research Center, Seattle, Washington 98109

Abstract

Although the amplified-in-breast cancer 1 (AIB1, SRC-3, ACTR or NCoA3) was defined as a coactivator for androgen receptor (AR) by *in vitro* studies, its role in AR-mediated prostate development and prostate cancer remained unexplored. We report here that AIB1 is expressed in the basal and stromal cells, but not in the epithelial cells of the normal mouse prostates. AIB1 deficiency only slightly delayed prostate growth and had no effect on androgen-dependent prostate regeneration, suggesting an unessential role of AIB1 in AR function in the prostate. Surprisingly, when prostate tumorigenesis was induced by the SV40 transgene in TRAMP mice, AIB1 expression was observed in certain epithelial cells of the prostate intraepithelial neoplasia (PIN) and well-differentiated carcinoma (WDC) and in almost all cells of the poorly differentiated carcinoma (PDC). After AIB1 was genetically inactivated in AIB1$^{-/-}$/TRAMP mice, the progression of prostate tumorigenesis in most AIB1$^{-/-}$/TRAMP mice was arrested at the WDC stage. WT/TRAMP mice developed progressive, multi-focal and metastatic prostate tumors and died between 25–34 weeks. In contrast, AIB1$^{-/-}$/TRAMP mice only exhibited PIN and early stage WDC by 39 weeks. AIB1$^{-/-}$/TRAMP prostates showed much lower cell proliferation than WT/TRAMP prostates. Most AIB1$^{-/-}$/TRAMP mice could survive more than 35 weeks and died with other types of tumors or unknown reasons. Our results indicate that induction of AIB1 expression in partially transformed epithelial cells is essential for progression of prostate tumorigenesis into PDC. Inhibition of AIB1 expression or function in the prostate epithelium may be a potential strategy to suppress prostate cancer initiation and progression.

Keywords

AIB1; SRC-3; overexpression; prostate cancer; tumor progression; TRAMP

Introduction

Prostate cancer is a major health problem as it was diagnosed in more than 230,000 American men in 2004 (1). Prostate cancer-related death is closely associated with dissemination and metastasis. Therefore, understanding prostate cancer progression prior to metastasis will improve therapeutic approaches. The progression of prostate cancer is believed to proceed through multiple steps, from prostatic intraepithelial neoplasia (PIN) to locally invasive

[*]Corresponding Author: Jianming Xu, Ph.D., Department of Molecular and Cellular Biology, Baylor College of Medicine One Baylor Plaza, Houston, TX, 77030, U.S.A. Phone: 713-798-6199; Fax: 713-798-3017; jxu@bcm.tmc.edu.
[3]Present address: Center for Inflammatory Diseases and Molecular Therapies, The University of Hong Kong, 21 Sassoon Road, Pokfulam, Hong Kong

carcinoma and finally to metastatic disease (2). Altered expression of oncogenes or tumor suppressor genes plays a vital role in prostate tumor initiation and progression.

The amplified–in-breast cancer 1 (AIB1, SRC-3 or NCoA3) is a transcriptional coactivator that was initially found overexpressed in breast and ovarian cancers (3–7). AIB1 is a member of the p160 steroid receptor coactivator (SRC) family that also contains SRC-1 and SRC-2 (TIF2 or GRIP1) (4,8). Biochemical and *in vitro* cellular experiments have demonstrated that the SRC family members can interact with steroid receptors in a ligand-dependent manner and enhance their transcriptional activities (9). In addition, AIB1 can interact with and coactivate a group of other p300/CBP-associated transcription factors, such as E2F1, Ets, NF-κB, and STAT (10–14).

In addition to breast and ovarian cancers, AIB1 is also overexpressed in endometrial and prostate cancers (5–7,15–17). The connection between AIB1 overexpression in steroid-promoted cancers and its coactivator activity for steroid receptors demonstrated by *in vitro* studies has strongly suggested that AIB1 plays an important role in hormonal promotion of tumorigenesis (6). However, recent studies also have found AIB1 amplification and overexpression in colorectal carcinomas, esophageal squamous cell carcinomas, gastric cancers, hepatocellular carcinomas (HCC), and pancreatic cancers (18–20), suggesting that AIB1 also participates in steroid hormone-independent cancers and contributes to tumorigenesis through transcription factors that are not steroid receptors.

Transgenic mouse models have been employed to dissect the role of AIB1 in cancer. Overexpression of AIB1 under the control of mouse mammary tumor virus (MMTV) LTR in transgenic mice leads to tumor formation in the mammary gland, lung, pituitary, and uterus (21), suggesting a sufficient role of AIB1 overexpression in tumorigenesis. To understand the physiological role of AIB1, our laboratory has generated $AIB1^{-/-}$ mice. These $AIB1^{-/-}$ mice exhibited growth retardation and impaired IGF signaling (22). Our laboratory also has shown that AIB1 deficiency suppressed v-Ha-ras-induced breast cancer initiation and progression in an ovarian hormone-independent manner, and $AIB1^{-/-}$ mice were resistant to chemical carcinogen-induced mammary tumorigenesis (23,24). These results imply that AIB1 participates in the initiation and/or progression of mammary tumors.

Emerging evidence suggests that AIB1 may also play a crucial role in prostate cancer. AIB1 was shown to be recruited to the prostate-specific antigen promoter by androgen receptor (AR) in cultured cells (25) and found to be overexpressed in human prostate tumors (16). Furthermore, AIB1 overexpression in these tumors correlated positively with cell proliferation and inversely with cell apoptosis. Conversely, knockdown of AIB1 in cultured prostate cancer cells decreased cell proliferation, delayed G1-S transition, and increased cell apoptosis (16). These findings suggest that AIB1 expression might be an important regulator for prostate tumorigenesis and for proliferation and survival of cultured prostate cancer cells. However, the tumorigenic stage-associated profile of AIB1 expression and the *in vivo* role of AIB1 expression in the entire process of prostate cancer initiation and progression remained to be characterized.

In this study, we have examined AIB1 expression and its developmental function in the mouse prostates and generated TRAMP (transgenic adenocarcinoma of the mouse prostate) mice with wild type (WT) or knockout AIB1 to investigate the role of AIB1 in prostate cancer initiation and progression. We show that AIB1 is only expressed in the stromal and basal cells of normal mouse prostates and is not required for androgen-stimulated luminal epithelial proliferation and prostate regeneration. AIB1 expression is induced in the transformed epithelial cells during prostate cancer progression. Most importantly, inactivation of AIB1 inhibits prostate tumor formation and arrests prostate tumor progression into poorly differentiated adenocarcinomas.

Thus, the tumorigenesis-induced AIB1 expression in the epithelial cells is essential for prostate cancer progression.

Materials and Methods

Mice

Animal protocols were approved by the Animal Care and Use Committee of Baylor College of Medicine. AIB1$^{-/-}$ mice were generated by replacing a portion of the AIB1 genomic the promoterless DNA with *LacZ* sequence as described (22). Because AIB1$^{-/-}$ mice with C57BL/6J strain background were lethal before birth, the AIB1 mutant colony was maintained by breeding heterozygous pairs with a mixed genetic background of 50% 129SvEv and 50% C57BL/6J. All offspring were genotyped by polymerase chain reaction (PCR) as described previously (22). The C57BL/6J TRAMP mice harboring the Probasin-SV40 Tag transgene were reported previously (26). Female C57BL/6J TRAMP mice were bred to AIB1$^{-/-}$ male mice with 50% C57BL/6J and 50% 129SvEv genetic background to obtain female AIB1$^{+/-}$/TRAMP and male AIB1$^{+/-}$ founders with a mixed genetic background of 75% C57BL/6J and 25% 129SvEv. Subsequently, these founder mice were bred to generate WT/TRAMP, AIB1$^{+/minus;}$/TRAMP and AIB1$^{-/-}$/TRAMP mice. This breeding strategy ensured that all experimental mice were heterozygous to the SV40 transgene and the mixed genetic background of 75% C57BL/6J and 25% 129SvEv was randomly distributed in all three genotype groups with equal opportunities. DNA was extracted from the ear biopsy and PCR was performed for genotypic analysis as described (22,26).

Measurement of prostate response to androgen

For all surgical procedures, mice were anesthetized by intraperitoneal (IP) injection of Avertin (2.5% in saline, 15 μl/g body weight). Mice (WT and AIB1$^{-/-}$ littermates) were castrated via a scrotal incision at 3 or 10 weeks of age. At 14 days after castration, 10-mm-long silastic capsules (Dow 02-285) filled with testosterone propionate (Sigma, St. Louis, MO) were implanted subcutaneously in the mice. At the time of sacrifice, all prostate lobes were collected and weighed. To explore detail structure, the prostate was incubated in 1% collagenase (Sigma, St. Louis, MO) for 10 minutes as described (27). The number of distant tips and branches were counted under a stereomicroscope (27).

Tissue examination and tumor grading

Prior to sacrifice, each mouse was anesthetized and weighed. All major organs were inspected for evidence of primary tumors and metastases. Necropsy notes and photographs were taken for documentation. At the time of sacrifice, the lower genitourinary (GU) tract, including the bladder, seminal vesicles, and all prostate lobes, was removed *en bloc*, and placed in a Petri dish containing phosphate buffered saline (PBS) to prevent desiccation. The bladder was emptied, and the tissues were gently blotted to remove excess PBS; then the entire GU tract was weighed. Under a dissecting microscope, the dorsal (DP), lateral (LP), ventral (VP), and anterior (AP) lobes of the prostate were separated and weighed. Periaortic lymph nodes were removed and weighed.

The following specimens were collected for histology: periaortic lymph nodes, liver, lung, seminal vesicles, and AP, DP, LP and VP lobes. All tissue samples were fixed in 10% (v/v) phosphate-buffered formalin for 12 h, dehydrated and embedded in paraffin. The tissues were histologically evaluated and graded, by examining the hematoxylin and eosin stained sections under a light microscope. The prostatic tissue was identified as normal, PIN, and well, moderately, or poorly differentiated adenocarcinomas (WDA, MDA and PDA), according to the grading system described previously (28).

Immunohistochemistry and X-Gal Staining

Immunohistochemistry (IHC) was performed as described (24). Sections were incubated with the following primary antibodies at 4 °C overnight: monoclonal anti-T antigen (BD Pharmingen, San Diego, CA), monoclonal anti-E-cadherin (BD Transduction Lab., San Diego, CA), monoclonal anti-cytokeratin 8 (CK8) (Developmental Studies Hybridoma Bank, Iowa City, IA), monoclonal anti-Ki67 (BD Pharmingen, San Diego, CA), polyclonal anti-AR and monoclonal anti-p63 (Santa Cruz Biotech., Santa Cruz, CA). X-gal staining was performed as previously described (22). X-Gal-stained sections were further fixed in formalin for 30 min before counterstaining with nuclear fast red for 2 min.

In situ Hybridization

Prostate tissues were fixed in 10% formalin, imbedded in paraffin and sectioned at 5 μm thickness. Re-hydrated sections were sequentially treated with 0.2 N HCl for 15 min at 70 °C, 2X SSC for 15 min at 70 °C, and 3 μg/ml proteinase K for 15 min at 37 °C. After washed in PBS containing 100 mM glycine, tissues were fixed in 4% paraformaldehyde for 20 min, acetylated with acetic anhydride in 0.1 M triethanolamine (pH 8) for 10 min, and washed with 5X SSC for 15 min. Pre-hybridization was carried out in 50% formamide, 5X SSC, 500 μg/ml salmon sperm DNA, 250 μg/ml tRNA and 5X Denhardt's solution for 4 hrs. The mouse AIB1 antisense probe and its negative control sense probe were described previously (29). The probes were made with the DIG RNA Labeling System (Roche Applied Science, Indianapolis, IN), treated with DNase I and checked on an agarose gel for quality control. Tissues were incubated overnight in the hybridization solution with probes at 65 °C and washed with 2X SSC and then 0.1X SSC at 65 °C. The sections were incubated in 100 mM Tris-HCl (pH 7.5) containing 2% blocking powder (Roche Applied Science, Indianapolis, IN) and 150 mM NaCl, and then in anti-Digoxgenin-AP (Roche Applied Science, Indianapolis, IN) at 1:1000 dilution for 2 hrs. Color was developed with NBT and BCIP in 100 mM Tris-HCl (pH 9.5), 100 mM NaCl and 50 mM $MgCl_2$ for 5 hrs at room temperature. Slides were washed in 10 mM Tris-HCl (pH 8) with 1 mM EDTA and mounted with Aquamount Solution (Lerner Lab., Pittsburgh, PA).

Immunoblotting analysis

For harvesting prostate samples at all ages for immunoblotting analysis, the entire individual prostate lobes with or without tumors were carefully dissected under stereomicroscope. For a tumor at 30 weeks, both peripheral and central areas of solid tumor tissues were collected for Western blot. Samples were immediately frozen in liquid nitrogen and stored at −80 °C till tissue lysates were prepared and immunoblotting analysis was performed as described previously (24). Primary antibodies used for immunoblotting analysis are as follows: monoclonal anti-T antigen, monoclonal anti-E-cadherin (BD Transduction Laboratory, San Diego, CA), monoclonal anti-SRC-1 (Biomeda, Foster City, CA), monoclonal anti-SRC-2 (BD Pharmingen, San Diego, CA), polyclonal anti-AR (Santa Cruz Biotechnology, Santa Cruz, CA), polyclonal anti-AIB1 (gift from Dr. R. Wu, Baylor College of Medicine), and polyclonal anti-β-actin (Sigma, St. Louis, MO).

Real-time RT-PCR

Total RNA was prepared from all prostate lobes of individual WT/TRAMP and $AIB1^{-/-}$/TRAMP mice. Real-time RT-PCR was performed with 150 ng RNA using the SYBR Green method. The PCR primers for SV40 t and T mRNAs were designed according to the GenBank sequence V01380. The common forward primer was 5′-tgctcatcaacctgactttgga. The reverse primer specific to SV40 t mRNA was 5′-caggccattgtttgcagtaca. The reverse primer specific to SV40 T mRNA was 5′-ctgctcccattcatcagttcc. As an epithelial RNA loading control, the relative mRNA concentration of the keratin 18 epithelial marker was also analyzed by real-time RT-PCR as described previously (30).

Measurement of proliferation and apoptosis

Ki67 immunoreactivity and the terminal dUTP nick end-labeling (TUNEL) assay were used to assess proliferation and apoptosis, respectively. At least 500 prostate cells were counted from at least three randomly selected areas from each slide (magnification: X400). The proliferation and apoptotic indices were expressed as a percentage of cells with dark brown nuclear staining to total cells. For each time point, at least three mice of each genotype were examined.

Results

AIB1 is not expressed in the luminal epithelial cells of the normal murine prostate

As an initial step to study the role of AIB1 in the prostate, we investigated its cell type-specific expression pattern by using the phenotypically normal AIB1$^{+/-}$ mice harboring a knock-in *LacZ* reporter. This AIB1 expression reporter was inserted into the second exon of the *AIB1* gene and its expression is under the control of the endogenous AIB1 promoter (22–24,31). If expressed, this reporter produces β-galacrosidase that is solely localized in the nucleus. We isolated prostate tissues from 10-week-old AIB1$^{+/-}$ mice and performed X-Gal staining. Positively stained blue cells were located at the peripheral region of the prostatic acini and in the stromal region (Fig. 1A, panel 1). When the basement membrane was visualized by laminin staining, the blue cells were found either in the stroma outside the basement membrane or between the basement membrane and the luminal epithelial layer (Fig. 1A, panel 3). The CK8-positive luminal epithelial cells were excluded from the blue color (Fig. 1A, panel 2) and blue cells between the basement membrane and the luminal epithelium were basal cells that specifically express p63 (Fig. 1A, panel 4). The prostate tissues from age-matched WT (AIB1$^{+/+}$) mice without *LacZ* reporter served as negative controls and showed no X-Gal staining signals (data not shown), validating the specificity of AIB1 promoter-controlled *LacZ* expression in AIB1$^{+/-}$ prostate. These results demonstrated that AIB1 is expressed in the stromal and basal cells but not in the luminal epithelial cells in the murine prostate. As AR is expressed in both stromal and epithelial cells of the prostate (32), these findings suggest that AIB1 is co-expressed with AR only in the stromal cells rather than the epithelial cells.

AIB1 has a subtle contribution to prostate growth and is not required for androgen-induced prostate growth

To investigate the role of AIB1 in prostate development, we examined prostatic morphogenesis in 3-, 5- and 10-week-old WT and AIB1$^{-/-}$ mice. We microdissected the prostate glands and counted the numbers of their distal tips and branches, which has been used as a classic index of prostate morphogenesis (27). The tip and branch numbers of AP and DP were similar in WT and AIB1$^{-/-}$ prostates at all ages examined. The tip and branch numbers of VP in AIB1$^{-/-}$ prostates were slightly less than those in WT prostates and their differences in tip number were statistically significant at 5 weeks and in branch number at 3 weeks. The tip and branch numbers of LP in AIB1$^{-/-}$ prostates were identical to those of WT prostates at 3 and 5 weeks, but were significantly less than those of WT prostates at 10 weeks (Fig. 1B and Supplementary Fig. 1A). These results suggest that AIB1 deficiency does not affect AP and DP morphogenesis, but slightly delays the growth of VP and LP.

Activation of AR in the stromal cells stimulates growth factor secretion and enhances prostate growth (33). Since AIB1 is expressed in the stromal cells, it might contribute to AR-dependent prostate growth. Therefore, we compared androgen response between AIB1$^{-/-}$ and WT prostates by the method described previously (34). In the first experiment, mice were castrated at the age of 3 weeks and treated with testosterone capsules for 7 or 14 days starting at the age of 5 weeks. Unexpectedly, testosterone replacement comparably increased the numbers of distal tips and branches of all prostate lobes (Supplementary Fig. 1B). In the second experiment,

mice were castrated at 10 weeks, maintained for 3 weeks to allow prostate repression, and then treated with testosterone capsules for 7 or 14 days to test androgen-stimulated regeneration. Again, AIB1$^{minus;/minus;}$ and WT prostates comparably responded to androgen depletion and replacement. The relative weights and the numbers of distal tips and branches of AP, VP, DP and LP were reduced significantly after castration and regenerated to the normal levels after testosterone treatment (Fig. 1C, and Supplementary Fig. 1C). These results imply that loss of AIB1 function did not affect androgen or AR-dependent prostate growth, maintenance and regeneration. Therefore, AIB1 is not an essential coactivator for AR-mediated normal prostate growth.

AIB1 expression is induced in prostate epithelial cells during tumorigenesis

To investigate the kinetic expression and the contribution of AIB1 during prostate carcinogenesis, we used the TRAMP model (26). In TRAMP mice, the minimal rat probasin promoter drives the SV40 expression (T and t antigens, PB-Tag) in prostate epithelium to induce adenocarcinoma. These TRAMP mice develop poorly differentiated invasive prostate adenocarcinomas within 30 weeks (28). We generated WT/TRAMP, AIB1$^{+/-}$/TRAMP and AIB1$^{-/-}$/TRAMP mice as described in the section of Materials and Methods (Fig. 2A). We isolated prostates from these mice and examined AIB1 protein by Western blot. AIB1 protein was undetectable in prostates of 12-week-old WT/TRAMP mice, but became detectable in prostates of 12- to 24-week-old WT/TRAMP mice and significantly increased in prostate tumors at 30 weeks (Fig. 2B). As expected, no AIB1 protein was detected in AIB1$^{-/-}$/TRAMP prostates at all time points, validating the absence of AIB1 in AIB1$^{-/-}$/TRAMP mice. These results demonstrate that AIB1 protein is overproduced in mouse prostate tumors.

Next, we addressed what cell type overproduced AIB1 during prostate cancer progression in these mice. We monitored the kinetic cell type-specific AIB1 expression during prostate carcinogenesis by X-Gal staining of cryosections from the AIB1$^{+/-}$/TRAMP prostates and tumors harboring the knock-in *LacZ* reporter (22). At the age of 12 weeks, AIB1 expression was exclusively found in stromal cells and basal cells, but not in the luminal epithelial cells in all four prostate lobes (Fig. 2C for DP and data not shown for other lobes). These results are consistent with the results observed in AIB1$^{+/-}$ mice (Fig. 1A), showing that AIB1 is not expressed in normal prostate luminal epithelium. Surprisingly, AIB1 expression appeared in certain transformed epithelial cells of PIN and WDA at 18 weeks and became more intensive in more than 60% of the epithelial cells of MDA at 24 weeks (Fig. 2C). At 30 weeks, very strong AIB1 expression signals were observed in most of the tumor cells of PDA (Fig. 2C). No X-Gal staining signal was observed in WT/TRAMP control prostates and tumor tissues that did not carry the knock-in *LacZ* reporter (Fig. 2C). *In situ* hybridization using an AIB1 antisense riboprobe confirmed the significant increase of AIB1 mRNA expression in MDA and PDA at 24 and 30 weeks. The specificity of the *in situ* hybridization was verified by using the sense riboprobe as negative control, which did not detect any signal in the same set of samples (Fig. 2D).

Taken together, these results demonstrated that AIB1 is induced in the luminal epithelial cells in early stages of prostate carcinogenesis and both the number of epithelial cells expressing AIB1 and the level of AIB1 expression in individual transformed epithelial cells are positively associated with the prostate cancer progression.

Loss of AIB1 suppresses prostate tumorigenesis and increases survival rate

To estimate the overall effect of AIB1 on oncogene-induced prostate tumorigenesis and survival, we studied more than 50 WT/TRAMP and AIB1$^{-/-}$/TRAMP mice for their prostate cancer-related mortality and tumor development. Owing to the large prostate tumor and occurrence of metastasis, WT/TRAMP mice (Fig. 3A) and AIB1$^{+/-}$/TRAMP mice (data not

shown) died between 16.8 and 35.6 weeks. 50% of WT/TRAMP mice died by the age of 26.8 weeks. In contrast, AIB1$^{-/-}$/TRAMP mice died between 28.1 and 50 weeks and about 50% of them lived longer than 39 weeks (Fig. 3A). Statistical analysis demonstrated that loss of AIB1 significantly prolonged the life span of AIB1$^{-/-}$/TRAMP mice compared to that of WT/TRAMP mice (Log-rank test, $p < 0.0001$).

More surprisingly, although all of the 20 WT/TRAMP mice examined at the time of necropsy developed large prostate tumors, there was no sign of prostate tumor in 14 out of 16 AIB1$^{-/-}$/TRAMP mice examined at the time of necropsy (Fig. 4A). The other 2 AIB1$^{-/-}$/TRAMP mice examined at 30 weeks of age developed small prostate tumors. Some of the prostate tumor-free AIB1$^{-/-}$/TRAMP mice developed other types of tumors, including tumors in throat (3 mice), kidneys (4 mice), seminal vesicle (3 mice) and liver (1 mouse). These mice died in coincidence with these tumors. Since aging mice also develop spontaneous tumors, we did not pursue these non-prostate tumors in this study. In addition, other AIB1$^{-/-}$/TRAMP mice exhibited normal genitourinary tract (GU), but their bodies were lean and they died with unknown reasons. These results indicate that AIB1 deficiency strongly suppresses prostate tumorigenesis.

To monitor prostate tumor growth in mice, body weight and the weight of GU were measured as a function of age and cancer progression (28). The averge body weight of AIB1$^{-/-}$/TRAMP mice was lighter than that of age-matched WT/TRAMP mice (Fig. 3B), which was expected since AIB1$^{-/-}$ non-TRAMP mice were smaller than WT mice (22). There was no significant difference in the ratio of kidney weight to body weight between WT/TRAMP and AIB1$^{-/-}$/TRAMP mice although their body weights were different (Fig. 3B), suggesting that relative organ weight can be used to monitor hyperplastic changes in these mice. The net GU weight in WT/TRAMP mice was significantly greater than that of AIB1$^{-/-}$/TRAMP littermates after 24 weeks of age ($P < 0.05$). The increase in relative GU weight as a function of time in each cohort followed the same trend as the increase in net GU weight (Fig. 3B). However, the net and relative GU weights in AIB1$^{-/-}$/TRAMP mice remained constant at all examined ages (Fig. 3B). A closer measurement revealed that the relative weights of individual prostate lobes showed a gradual increase from the age of 8 weeks to 30 weeks (Fig 3B). These results demonstrated that WT/TRAMP prostate tumors grow rapidly but AIB1$^{-/-}$/TRAMP prostates only exhibit a small hyperplastic growth.

In addition, metastatic lesions in the seminal vesicle, periaortic lymph nodes, lung, and liver were observed in WT/TRAMP mice but not in AIB1$^{-/-}$/TRAMP mice, including the two 30-week-old AIB1$^{-/-}$/TRAMP mice with prostate tumors. Following the development of metastasis in WT/TRAMP mice, the relative weights of periaortic lymph nodes were significantly increased after the age of 24 weeks. In contrast, the relative weights of AIB1$^{-/-}$/TRAMP lymph nodes remained constant from the age of 8 to 30 weeks (Fig. 3B). Histological examination of lymph nodes also confirmed the same finding. These results suggest that loss of AIB1 inhibits both prostate tumor formation and metastasis.

Inactivation of AIB1 impedes prostate cancer progression

Morphologically, prostate cancer progression consists of multiple stages from PIN to WD, MD and PD carcinomas. To determine how AIB1 deficiency affected prostate cancer initiation and progression, we performed histopathological examination. As evidenced by epithelial hyperplasia and the presence of an intact basal-cell layer, PIN was developed in almost all DP, LP and VP lobes in both WT/TRAMP and AIB1$^{-/-}$/TRAMP mice from 8 to 12 weeks of age (Fig. 4B and data not shown). At 18 weeks, high-grade PIN and WDA were observed in DP, LP and VP lobes in WT/TRAMP mice ($n = 5$) as evidenced by an increase in small glands, but only PIN was observed in DP, LP and VP lobes in AIB1$^{-/-}$/TRAMP mice ($n = 5$). By 24 weeks, 3 of 6 WT/TRAMP mice developed high-grade WDA or MDA and had invasive foci. Stromal

thickening and active cell proliferation through the basement membranes of small glands were seen at these stages. The other 3 mice developed PDA characteristic of anaplastic sheets of tumor cells. Interestingly, all AIB1$^{-/-}$/TRAMP mice (n = 5) only developed high-grade PIN in DP, LP and VP lobes (Fig. 4B and data now shown). By 30 weeks, all of WT/TRAMP mice (n = 6) displayed PDA. In contrast, none of AIB1$^{-/-}$/TRAMP mice (n = 5) had PDA and they only formed early-stage WDA (Fig. 4B and data not shown). These histopathological results are consistent with the morphological observation showing that most AIB1$^{-/-}$/TRAMP mice did not develop visible prostate tumors. Taken together, these findings suggest that inactivation of AIB1 arrests prostate cancer progression at the stage of WDA.

The above notion is further supported by the expression of epithelial markers. As prostate carcinomas progress, the epithelial cells appear to lose epithelial differentiation and acquire more mesenchymal morphology and metastatic potential (28). In clinical prostate cancer, well differentiated tumors typically retain expression of E-cadherin while poorly differentiated tumors show reduced or abnormal expression (35,36). Similar to clinical cancer, abundant E-cadherin was detected in PIN and WDA lesions in all prostate lobes of 18- and 24-week-old WT/TRAMP mice, but E-cadherin was significantly reduced or absent in PDA in 30-week-old WT/TRAMP mice (Fig. 4C and data not shown). However, E-cadherin was steadily detected in all prostate lobes, PIN and WDA in AIB1$^{-/-}$/TRAMP mice at all ages (Fig. 4C and data now shown). Western blot analysis of tissue lysates prepared from all prostate lobes confirmed that E-cadherin was drastically reduced in the WT/TRAMP prostate tumors, but not reduced in the AIB1$^{-/-}$/TRAMP prostates or tumors of 30-week-old mice (Fig. 5A). Similar results were also observed for another epithelial marker, CK8. In normal prostate, CK8 is expressed exclusively in the luminal epithelia (28,37). In the poorly differentiated carcinomas of 30-week-old WT/TRAMP mice, CK8 staining was weak or absent. Interestingly, CK8 was still expressed in the prostates or tumors of 30-week-old AIB1$^{-/-}$/TRAMP mice (Supplementary Fig. 2). These results demonstrate that the epithelial property is maintained in AIB1$^{-/-}$/TRAMP prostatic epithelium and tumors and thereby further support the conclusion that AIB1 deficiency impedes prostate tumor progression at the WDA stage.

Effects of AIB1 deficiency on the expression of SV40 T antigen, AR, SRC-1 and SRC-2

To follow the PB-Tag transgene expression, sections representing various stages of cancer progression were immunostained with an antibody specific for SV40 T antigen. As expected for the negative control, T antigen was undetectable in the prostates of WT and AIB1$^{-/-}$ mice (data not shown). In WT/TRAMP and AIB1$^{-/-}$/TRAMP mice, the T antigen immunoreactivity was comparable in the prostatic epithelial cells as early as 8 weeks of age. The T antigen continued to express in prostatic epithelium and tumor cells at all examined ages (18–30 weeks) in both types of mice. The T antigen immunoreactivity was similar in individual epithelial cells of DP, LP and VP lobes in WT/TRAMP and AIB1$^{-/-}$/TRAMP mice through all ages except that the T antigen expression was largely reduced in some of the PDA cells in 30-week-old WT/TRAMP mice (Fig. 4D and data not shown). To quantify the amount of SV40 t and T mRNA expression, we performed real-time RT-PCR analysis using RNA samples prepared from all prostate lobes of 18-week-old WT/TRAMP and AIB1$^{-/-}$/TRAMP mice. Since the PB-Tag transgene was specifically expressed in the prostate epithelial cells, the relative expression levels of SV40 mRNAs were normalized to the levels of keratin 18 mRNA that is also specifically expressed in the epithelial cells. Our measurements revealed that the SV40 t mRNA was expressed about two fold higher than the SV40 T mRNA in both WT/TRAMP and AIB1$^{-/-}$/TRAMP prostates. However, the expression levels of both mRNA pieces in WT/TRAMP prostates were the same as that in AIB1$^{-/-}$/TRAMP prostates (Fig. 5B). Furthermore, we performed Western blot analysis with 3 sets of independent prostate samples isolated from 12-, 18-, 24- and 30-week-old WT/TRAMP and AIB1$^{-/-}$/TRAMP mice and normalized the band intensity to CK8, an epithelial cell-specific protein. These assays revealed that the T

antigen protein levels were comparable in WT/TRAMP and AIB1$^{-/-}$/TRAMP prostatic epithelial cells (Fig. 5C). These results clearly demonstrate that AIB1 deficiency does not affect the PB-Tag transgene expression in the prostate epithelial cells.

We also analyzed the expression levels of AR and the other two SRC family members (SRC-1 and SRC-2) in the prostates of WT/TRAMP and AIB1$^{-/-}$/TRAMP mice with different ages by Western blot analysis of 3 sets of samples. Although their protein levels were variable among different mice, the average amounts of AR, SRC-1 and SRC-2 were not significantly different between WT/TRAMP and AIB1$^{-/-}$/TRAMP mice (Fig. 5D). These results suggest that AIB1 deficiency has no obvious effects on the expression of AR, SRC-1 and SRC-2 in the prostate.

Inactivation of AIB1 reduces cell proliferation

Prostate tumor progression usually involves alteration of cell proliferation and apoptosis (38–41). To determine possible changes in cell proliferation and apoptosis leading to the inhibition of prostate tumor progression in AIB1$^{-/-}$/TRAMP mice, we performed IHC with an antibody against the Ki-67, a S-phase marker, to detect proliferative cells and TUNEL assay to detect apoptotic cells. These assays were carried out at various ages in coordination with AIB1 expression analysis. The percentages of Ki-67-positive cells in VP, DP, and LP were high in the prostate epithelium of 8-week-old WT/TRAMP and AIB1$^{-/-}$/TRAMP mice because of their rapid growth at puberty (Fig. 6A). In WT/TRAMP mice, proliferation indices in VP, DP, and LP decreased at 12 weeks as the prostate matured, but significantly increased during the progression of prostate cancer from 18 to 24 weeks. However, in AIB1$^{-/-}$/TRAMP mice the proliferation indices were significantly lower in VP and LP at 12 weeks and in VP, DP and LP at 18 and 24 weeks compared with age-matched WT/TRAMP mice. At 30 weeks, the proliferation indices remained high in WT/TRAMP tumors while large tumors made it impossible to isolate individual prostate lobes from these mice for proliferation assay. The proliferation indices remained unchanged in 30-week-old AIB1$^{-/-}$/TRAMP mice compared with younger AIB1$^{-/-}$/TRAMP mice (Fig. 6A). The proliferation rate in the AP lobe showed little changes because the PB-Tag transgene had little expression in the AP lobe due to a limited PB promoter activity. Interestingly, the apoptotic cell indices were as low as 1–2% in all lobes of both WT/TRAMP and AIB1$^{-/-}$/TRAMP prostates and maintained at similar levels at all examined ages, except that high apoptotic indices were observed in the central area of large tumors with extensive cell death in 30-week-old WT/TRAMP mice (Supplementary Fig. 3). In summary, these results demonstrate that loss of AIB1 function significantly decreases prostate epithelial and tumor cell proliferation induced by SV40-triggered tumorigenesis, but it has little effect on cell apoptosis.

Discussion

AIB1 has garnered extensive attention because of its overexpression and possible roles in human breast, esophageal, gastric, ovarian, pancreatic and prostate cancers (3,4,6,42). In certain prostate tumors, AIB1 was found overexpressed and its overexpression was associated with the disease recurrence (17,43). Conversely, the knockdown of AIB1 was shown to inhibit proliferation and promote apoptosis of cultured prostate cancer cells both positive and negative to AR (16). Although these studies suggest that AIB1 might play an important role in prostate cancer, the physiological function of AIB1 in the androgen-regulated prostate development, the AIB1 expression profile associated with prostate cancer progression stages and the *in vivo* role of AIB1 in prostate cancer initiation and progression were not established.

This study demonstrates that AIB1 is expressed in the stromal and basal cells rather than luminal epithelial cells in the normal murine prostate. Genetic deletion of AIB1 only slightly affects the prostate morphogenesis during puberty but has no obvious effects on the prostate regression following androgen withdrawal and the prostate regeneration after androgen

replacement. These findings suggest that AIB1 is not an essential coactivator for AR in the normal prostate, this notion is further supported by the fact that the SV40 transgene expression driven by the androgen-responsive probasin promoter is identical in individual prostatic epithelial cells of WT/TRAMP and AIB1$^{-/-}$/TRAMP mice.

More importantly, this study further demonstrates that in the prostate of WT/TRAMP mice, AIB1 expression is progressively induced in the SV40 antigen-transformed epithelial cells, which appears initially in a small cell population at the late PIN stage, subsequently in most of the transformed epithelial cells from WDA to MDA stages, and finally in almost all of the tumor cells at the PDA stage (Fig. 6C). Inactivation of AIB1 in the prostate of AIB1$^{-/-}$/TRAMP mice significantly extends their lifespan, greatly reduces the epithelial proliferation and tumor burden, maintains the expression of epithelial markers such as E-cadherin and CK8, and results in a blockade of prostate cancer progression at the WDA stage (Fig. 6C). These results indicate that AIB1 expression in the prostate epithelial cells induced by the SV40 antigen-triggered cellular transformation is essential for prostate tumor growth and progression. Therefore, AIB1 may be a biomarker for prostate cancer progression and a possible therapeutic molecular target for prostate cancer treatment.

The AIB1$^{+/-}$ mouse line harboring the knock-in *LacZ* indicator for the endogenous AIB1 promoter activity is a sensitive and powerful tool to indicate temporal and spatial patterns of AIB1 expression. It has been faithfully used to detect AIB1 expression in the brain hippocampus, mammary epithelial cells, vascular smooth muscle and endothelial cells, uterine smooth muscle cells and oocytes (22–24,31). This mouse line is particularly useful in the case encountered in this study where AIB1 expression is low and all available AIB1 antibodies failed to reliably detect AIB1 protein in the mouse prostate by IHC. The AIB1 expression patterns indicated by the *LacZ* reporter in the mouse prostates and tumors are consistent with the results of *in situ* hybridization in the same sets of tissues and with the results observed in the human prostate and prostate tumors. In the “normal” human prostatic epithelium, AIB1 expression is also undetectable or at very low levels (16). In human prostate carcinomas and cancer cells, AIB1 is overproduced (17,43). Importantly, this study provided new molecular genetic evidence showing that AIB1 expression is induced after the initiation of prostate carcinogenesis and during a period from severe PIN to WD carcinoma stages.

Since the SV40 transgene is expressed virtually in all epithelial cells of the DP, LP and VP lobes as early as 8 weeks of age and AIB1 is induced in a subpopulation of transformed prostatic epithelial cells as late as 18 weeks of age, the induction of AIB1 expression is not an immediate consequence of SV40 expression. Instead, it might be a consequence of progressive activation of cell growth signaling pathways responsible for prostate cancer progression. Although it is unclear what is the direct factor that switches on AIB1 expression in the transformed epithelium, recent studies have shown that AIB1 is a coactivator of E2F1 and E2F1 overactivation can stimulate AIB1 overexpression (12,44,45), which forms a positive feedback regulatory loop to maintain AIB1 overexpression and to enhance cell proliferation (45). Therefore, the SV40-induced cellular transformation may result in E2F1 overactivation and cause AIB1 overexpression in the transformed prostate epithelial cells.

The fact that 2 out of 16 (12.5%) examined AIB1$^{-/-}$/TRAMP mice still developed prostate tumors indicates that AIB1 deficiency do not arrest all prostate cancer progression induced by the SV40 antigen. Our data showed that SV40 antigen was expressed in most epithelial cells starting at 8 weeks, but only some of the epithelial cells became transformed and grew into tumors at a later stage. This observation suggests that the SV40 antigens alone are not sufficient to induce prostate cancer, and SV40 antigen-induced accumulation of genetic and/or epigenetic alterations is responsible for the development of prostate cancers. Since individual tumors might be induced by different signaling pathways activated by different combinations of

genetic/epigenetic changes, the molecular mechanisms leading to the development of SV40-induced prostate tumors should include AIB1-dependent and independent pathways. AIB1 deficiency should inhibit AIB1-dependent pathways and tumor progression, but would not block AIB1-independent pathways and tumor progression. This notion is further supported by multiple lines of evidence showing that AIB1 is amplified and overexpressed in some but not all of the human breast and prostate tumors (6,16).

Our results showed that removal of AIB1 prevents SV40-transformed prostate epithelial cells from overproliferation and arrests prostate tumor development and progression in most AIB1$^{-/-}$/TRAMP mice. This dramatic impact of AIB1 deficiency should be attributed to the involvement of AIB1 in multiple regulatory pathways. First, since previous studies using biochemical analysis and manipulated cell lines have shown that overexpressed AIB1 could enhance AR activity, Akt activity and promote cell proliferation (18,19), one could think of the possibility that the oncogenesis-induced AIB1 expression in the transformed epithelial cells might serve as a coactivator for AR to promote cell proliferation and carcinogenesis. However, this possibility is damped by the results showing that AIB1 expressed in the basal and stromal cells was not required for androgen-stimulated prostate growth and regeneration and AIB1 expressed in the transformed prostate epithelial cells of WT/TAMP mice did not alter the expression level of the SV40 transgene directed by the androgen-responsive probasin promoter. Second, our previous studies have shown that AIB1 deficiency inhibits overactivation of IGF-I signaling pathways during mammary tumorigenesis by preventing IGF-I, IRS-1, IRS-2 and cycline D1 overexpression and Akt overactivation (23,24). Other studies have also shown that overexpression of AIB1 in transgenic mice significantly stimulates IGF-I signaling pathways and results in tumors in the mammary gland, lung, pituitary and uterus (21). Therefore, AIB1 deficiency may suppress the overactivation of IGF-I signaling pathways induced by the prostate epithelial transformation and inhibit prostate cancer progression. Third, AIB1 has been found to increase cell size and survival capability of prostate cancer cells in culture (16,43). Finally, AIB1 can interact with and coactivate a group of transcription factors including AP-1, Ets factors, NF-κB and E2F1 known to be important for cell proliferation, survival and carcinogenesis, (11,12,14,44,46–48). Taken together, the blockade of prostate cancer progression by AIB1 deficiency should be a combined result from the effects of AIB1 deficiency on multiple signaling pathways. Additional investigation of the major pathways and target genes regulated by AIB1 should provide new insight into the understanding of molecular mechanisms and gene networks that govern prostate cancer progression.

Our analysis did not find appreciable change of cell apoptosis during prostate cancer progression in WT/TRAMP and AIB1$^{-/-}$/TRAMP mice, which was different from the results observed in the cultured prostate cancer cells where AIB1 depletion caused extensive apoptosis (16). Other studies showing a delay in tumor progression in TRAMP mice also demonstrated an elevation of apoptosis (38–41). These differences may be explained by the essential role of AIB1 in prostate cancer progression. In other words, once the transformed prostate epithelial cells depend on AIB1 expression to progress to an advanced malignant stage, these tumor cells may become more dependent on AIB1 to survive. Depletion of AIB1 in these malignant cancer cells such as the cultured prostate cancer cell lines would reduce their viability and result in apoptosis (16). In our *in vivo* model, the genetic ablation of AIB1 arrests prostate tumor progression at the MDA stage. Since AIB1 is never expressed in the AIB1$^{-/-}$/TRAMP prostate epithelial cells, the partially transformed AIB1$^{-/-}$/TRAMP epithelial cells still express epithelial cell markers and should be in an AIB1-independent status for survival. Thus, no obvious cell apoptosis would happen.

In summary, we have explored the role of AIB1 in prostate cancer progression using the bi-transgenic mouse models. We demonstrate here that AIB1 protein is indeed induced by prostate oncogenesis and this induction of AIB1 overproduction is required for prostate cancer

progression. Our results provide the first molecular genetic evidence that AIB1 regulates a gene expression program that promotes the prostate cancer progression from carcinoma *in situ* to invasive carcinoma. Future studies designed to understand the complex molecular mechanisms and to characterize AIB1-regulated genes responsible for promotion of prostate cancer progression should further advance our knowledge to understand and control human prostate cancer.

Supplementary Material

Refer to Web version on PubMed Central for supplementary material.

Acknowledgments

We thank Dr. Hao Zhang for professional assistance, and Drs. Daniel and Marvin L. Meistrich for the advice about silastic capsule implantation procedures. This work was partially supported by CA119689, CA112403 and DK58242 NIH grants to J.X. and an American Heart Association Career Award (0330144N) to A.C.K.C. J.X. is a recipient of the American Cancer Society Scholar Award (RSG-05-082-01-TBE).

References

1. Cooperberg MR, Moul JW, Carroll PR. The changing face of prostate cancer. J Clin Oncol 2005;23:8146–51. [PubMed: 16278465]
2. Nelson WG, De Marzo AM, Isaacs WB. Prostate cancer. N Engl J Med 2003;349(4):366–81. [PubMed: 12878745]
3. Liao L, Kuang SQ, Yuan Y, Gonzalez SM, O'Malley BW, Xu J. Molecular structure and biological function of the cancer-amplified nuclear receptor coactivator SRC-3/AIB1. J Steroid Biochem Mol Biol 2002;83:3–14. [PubMed: 12650696]
4. Xu J, Li Q. Review of the in vivo functions of the p160 steroid receptor coactivator family. Mol Endocrinol 2003;17:1681–92. [PubMed: 12805412]
5. List HJ, Reiter R, Singh B, Wellstein A, Riegel AT. Expression of the nuclear coactivator AIB1 in normal and malignant breast tissue. Breast Cancer Res Treat 2001;68:21–8. [PubMed: 11678305]
6. Anzick SL, Kononen J, Walker RL, et al. AIB1, a steroid receptor coactivator amplified in breast and ovarian cancer. Science 1997;277:965–8. [PubMed: 9252329]
7. Bautista S, Valles H, Walker RL, et al. In breast cancer, amplification of the steroid receptor coactivator gene AIB1 is correlated with estrogen and progesterone receptor positivity. Clin Cancer Res 1998;4:2925–9. [PubMed: 9865902]
8. McKenna NJ, O'Malley BW. Combinatorial control of gene expression by nuclear receptors and coregulators. Cell 2002;108:465–74. [PubMed: 11909518]
9. McKenna NJ, Xu J, Nawaz Z, Tsai SY, Tsai MJ, O'Malley BW. Nuclear receptor coactivators: multiple enzymes, multiple complexes, multiple functions. J Steroid Biochem Mol Biol 1999;69:3–12. [PubMed: 10418975]
10. Arimura A, vn Peer M, Schroder AJ, Rothman PB. The transcriptional co-activator p/CIP (NCoA-3) is up-regulated by STAT6 and serves as a positive regulator of transcriptional activation by STAT6. J Biol Chem 2004;279:31105–12. [PubMed: 15145939]
11. Myers E, Hill AD, Kelly G, et al. Associations and interactions between Ets-1 and Ets-2 and coregulatory proteins, SRC-1, AIB1, and NCoR in breast cancer. Clin Cancer Res 2005;11:2111–22. [PubMed: 15788656]
12. Louie MC, Zou JX, Rabinovich A, Chen HW. ACTR/AIB1 functions as an E2F1 coactivator to promote breast cancer cell proliferation and antiestrogen resistance. Mol Cell Biol 2004;24:5157–71. [PubMed: 15169882]
13. Torchia J, Rose DW, Inostroza J, et al. The transcriptional co-activator p/CIP binds CBP and mediates nuclear-receptor function. Nature 1997;387:677–84. [PubMed: 9192892]
14. Werbajh S, Nojek I, Lanz R, Costas MA. RAC-3 is a NF-kappa B coactivator. FEBS Lett 2000;485:195–9. [PubMed: 11094166]

15. Glaeser M, Floetotto T, Hanstein B, Beckmann MW, Niederacher D. Gene amplification and expression of the steroid receptor coactivator SRC3 (AIB1) in sporadic breast and endometrial carcinomas. Horm Metab Res 2001;33:121–6. [PubMed: 11355743]
16. Zhou HJ, Yan J, Luo W, et al. SRC-3 is required for prostate cancer cell proliferation and survival. Cancer Res 2005;65:7976–83. [PubMed: 16140970]
17. Gnanapragasam VJ, Leung HY, Pulimood AS, Neal DE, Robson CN. Expression of RAC 3, a steroid hormone receptor co-activator in prostate cancer. Br J Cancer 2001;85:1928–36. [PubMed: 11747336]
18. Wang Y, Wu MC, Sham JS, Zhang W, Wu WQ, Guan XY. Prognostic significance of c-myc and AIB1 amplification in hepatocellular carcinoma. A broad survey using high-throughput tissue microarray. Cancer 2002;95:2346–52. [PubMed: 12436441]
19. Sakakura C, Hagiwara A, Yasuoka R, et al. Amplification and over-expression of the AIB1 nuclear receptor co-activator gene in primary gastric cancers. Int J Cancer 2000;89:217–23. [PubMed: 10861496]
20. Ghadimi BM, Schrock E, Walker RL, et al. Specific chromosomal aberrations and amplification of the AIB1 nuclear receptor coactivator gene in pancreatic carcinomas. Am J Pathol 1999;154:525–36. [PubMed: 10027410]
21. Torres-Arzayus MI, Font de Mora J, Yuan J, et al. High tumor incidence and activation of the PI3K/AKT pathway in transgenic mice define AIB1 as an oncogene. Cancer Cell 2004;6:263–74. [PubMed: 15380517]
22. Xu J, Liao L, Ning G, Yoshida-Komiya H, Deng C, O'Malley BW. The steroid receptor coactivator SRC-3 (p/CIP/RAC3/AIB1/ACTR/TRAM-1) is required for normal growth, puberty, female reproductive function, and mammary gland development. Proc Natl Acad Sci U S A 2000;97:6379–84. [PubMed: 10823921]
23. Kuang SQ, Liao L, Zhang H, Lee AV, O'Malley BW, Xu J. AIB1/SRC-3 deficiency affects insulin-like growth factor I signaling pathway and suppresses v-Ha-ras-induced breast cancer initiation and progression in mice. Cancer Res 2004;64:1875–85. [PubMed: 14996752]
24. Kuang SQ, Liao L, Wang S, Medina D, O'Malley BW, Xu J. Mice lacking the amplified in breast cancer 1/steroid receptor coactivator-3 are resistant to chemical carcinogen-induced mammary tumorigenesis. Cancer Res 2005;65:7993–8002. [PubMed: 16140972]
25. Louie MC, Yang HQ, Ma AH, et al. Androgen-induced recruitment of RNA polymerase II to a nuclear receptor-p160 coactivator complex. Proc Natl Acad Sci U S A 2003;100:2226–30. [PubMed: 12589022]
26. Gingrich JR, Barrios RJ, Morton RA, et al. Metastatic prostate cancer in a transgenic mouse. Cancer Res 1996;56:4096–102. [PubMed: 8797572]
27. Sugimura Y, Cunha GR, Donjacour AA. Morphogenesis of ductal networks in the mouse prostate. Biol Reprod 1986;34:961–71. [PubMed: 3730488]
28. Kaplan-Lefko PJ, Chen TM, Ittmann MM, et al. Pathobiology of autochthonous prostate cancer in a pre-clinical transgenic mouse model. Prostate 2003;55:219–37. [PubMed: 12692788]
29. Nishihara E, Yoshida-Komiya H, Chan CS, et al. SRC-1 null mice exhibit moderate motor dysfunction and delayed development of cerebellar Purkinje cells. J Neurosci 2003;23:213–22. [PubMed: 12514218]
30. Mussi P, Liao L, Park SE, et al. Haploinsufficiency of the corepressor of estrogen receptor activity (REA) enhances estrogen receptor function in the mammary gland. Proc Natl Acad Sci U S A 2006;103:16716–21. [PubMed: 17065319]
31. Yuan Y, Liao L, Tulis DA, Xu J. Steroid receptor coactivator-3 is required for inhibition of neointima formation by estrogen. Circulation 2002;105:2653–9. [PubMed: 12045172]
32. Gioeli D. Signal transduction in prostate cancer progression. Clin Sci (Lond) 2005;108:293–308. [PubMed: 15603554]
33. Long RM, Morrissey C, Fitzpatrick JM, Watson RW. Prostate epithelial cell differentiation and its relevance to the understanding of prostate cancer therapies. Clin Sci (Lond) 2005;108:1–11. [PubMed: 15384949]

34. Sugimura Y, Cunha GR, Donjacour AA. Morphological and histological study of castration-induced degeneration and androgen-induced regeneration in the mouse prostate. Biol Reprod 1986;34:973–83. [PubMed: 3730489]
35. Tomita K, van Bokhoven A, van Leenders GJ, et al. Cadherin switching in human prostate cancer progression. Cancer Res 2000;60:3650–4. [PubMed: 10910081]
36. De Marzo AM, Knudsen B, Chan-Tack K, Epstein JI. E-cadherin expression as a marker of tumor aggressiveness in routinely processed radical prostatectomy specimens. Urology 1999;53:707–13. [PubMed: 10197845]
37. Wang Y, Hayward S, Cao M, Thayer K, Cunha G. Cell differentiation lineage in the prostate. Differentiation 2001;68:270–9. [PubMed: 11776479]
38. Huss WJ, Lai L, Barrios RJ, Hirschi KK, Greenberg NM. Retinoic acid slows progression and promotes apoptosis of spontaneous prostate cancer. Prostate 2004;61:142–52. [PubMed: 15305337]
39. Narayanan BA, Narayanan NK, Pittman B, Reddy BS. Regression of mouse prostatic intraepithelial neoplasia by nonsteroidal anti-inflammatory drugs in the transgenic adenocarcinoma mouse prostate model. Clin Cancer Res 2004;10:7727–37. [PubMed: 15570007]
40. Gupta S, Adhami VM, Subbarayan M, et al. Suppression of prostate carcinogenesis by dietary supplementation of celecoxib in transgenic adenocarcinoma of the mouse prostate model. Cancer Res 2004;64:3334–43. [PubMed: 15126378]
41. Williams TM, Hassan GS, Li J, et al. Caveolin-1 promotes tumor progression in an autochthonous mouse model of prostate cancer: genetic ablation of Cav-1 delays advanced prostate tumor development in tramp mice. J Biol Chem 2005;280:25134–45. [PubMed: 15802273]
42. Yan J, Tsai SY, Tsai MJ. SRC-3/AIB1: transcriptional coactivator in oncogenesis. Acta Pharmacol Sin 2006;27:387–94. [PubMed: 16539836]
43. Zhou G, Hashimoto Y, Kwak I, Tsai SY, Tsai MJ. Role of the steroid receptor coactivator SRC-3 in cell growth. Mol Cell Biol 2003;23:7742–55. [PubMed: 14560019]
44. Louie MC, Revenko AS, Zou JX, Yao J, Chen HW. Direct control of cell cycle gene expression by proto-oncogene product ACTR, and its autoregulation underlies its transforming activity. Mol Cell Biol 2006;26:3810–23. [PubMed: 16648476]
45. Mussi P, Yu C, O'Malley BW, Xu J. Stimulation of Steroid Receptor Coactivator-3 (SRC-3) Gene Overexpression by a Positive Regulatory Loop of E2F1 and SRC-3. Mol Endocrinol 2006;20:3105–19. [PubMed: 16916939]
46. Lee SK, Kim HJ, Kim JW, Lee JW. Steroid receptor coactivator-1 and its family members differentially regulate transactivation by the tumor suppressor protein p53. Mol Endocrinol 1999;13:1924–33. [PubMed: 10551785]
47. Goel A, Janknecht R. Concerted activation of ETS protein ER81 by p160 coactivators, the acetyltransferase p300 and the receptor tyrosine kinase HER2/Neu. J Biol Chem 2004;279:14909–16. [PubMed: 14747462]
48. Wu RC, Qin J, Hashimoto Y, et al. Regulation of SRC-3 (pCIP/ACTR/AIB-1/RAC-3/TRAM-1) Coactivator activity by I kappa B kinase. Mol Cell Biol 2002;22:3549–61. [PubMed: 11971985]

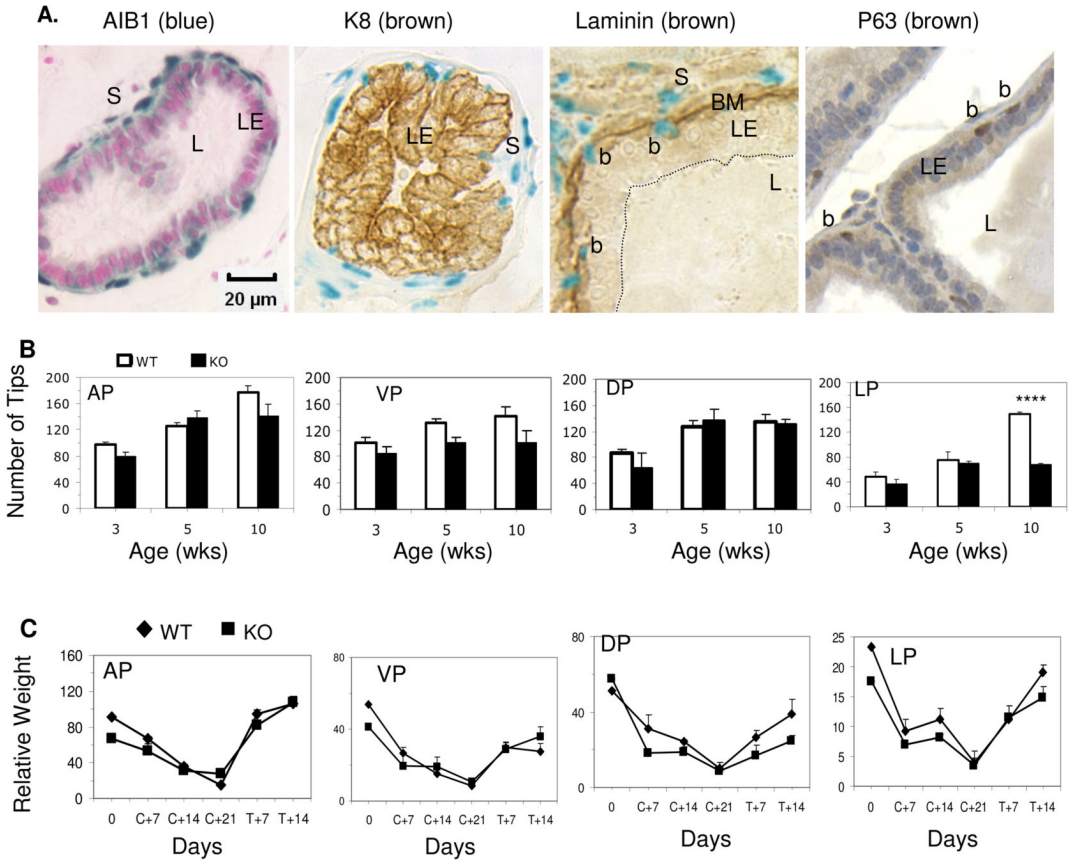

Fig. 1. AIB1 expression and function in the murine prostate

A. AIB1 expression in the basal and stromal cells. AIB1 expression is revealed by X-gal staining (blue color in the nuclei in panels 1–3). No blue color is located in the nuclei of luminal epithelial (LE) cells that are positively stained for CK8 (panel 2). Some blue cells are located in the stromal (S) region outside of the basement membrane (BM) (panel 3). BM is highlighted by laminin immunostaining. Other blue cells are basal cells (b) that are located between BM and the LE layer (panel 3) and are positively stained for p63 (panel 4). Similar results were observed in AP, VP, DP and LP lobes. L, lumen.

B. Comparison of prostate growth in WT and AIB1$^{-/-}$ (KO) mice. The four lobes of prostate were micro-dissected from 4 or more WT and AIB1$^{-/-}$ mice at the indicated ages. The numbers of distal tips for individual lobes were counted and presented as Mean ± SEM. ****, $P < 0.001$ by unpaired t test.

C. Comparison of prostate response to androgen in adult WT and AIB1$^{-/-}$ (KO) mice. 10-week-old mice (n = 6 for each time point) were castrated on day 0 and testosterone was replaced on day 21 (C+21) until day 35 (T+14). Prostate and body weights were measured at indicated time points and presented as relative prostate weight (Mean ± SEM). Relative weight was calculated by (prostate weight × 100)/body weight.

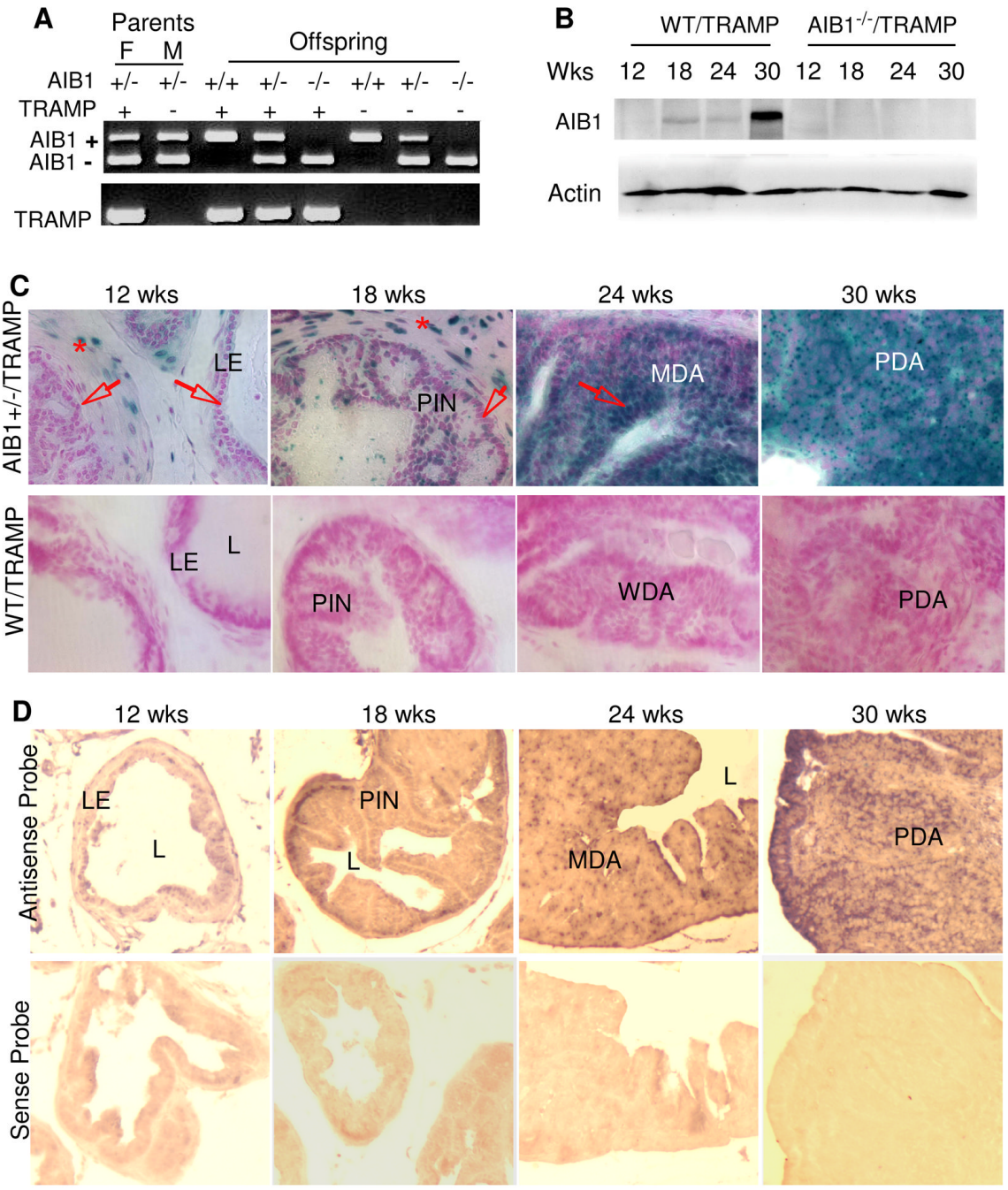

Fig. 2. AIB1 expression is induced in prostate epithelial cells during tumorigenesis in TRAMP mice

A. Gel images showing AIB1$^{+/+}$/TRAMP, AIB1$^{+/-}$/TRAMP and AIB1$^{-/-}$/TRAMP mouse genotypes analyzed by PCR. The upper panel shows the detected AIB1 WT (450 bp) and mutant allele (230bp). The lower panel shows the detected TRAMP transgene (600 bp). F and M indicate a breeding pair of female and male mice.

B. Western blot analysis of AIB1 in prostates and tumors in WT/TRAMP and AIB1$^{-/-}$/TRAMP mice with indicated ages. A significant increase of AIB1 protein is associated with the progression of prostate tumorigenesis in WT/TRAMP mice. β-actin was used as a loading control.

C. Analysis of AIB1 expression during prostate tumor initiation and progression. All prostate lobes were isolated from AIB1$^{+/-}$/TRAMP mice with a *LacZ* knock-in reporter and from WT/TRAMP mice without the reporter (negative control for X-Gal staining) at indicated ages. X-Gal staining was performed on cryosections. Note that AIB1 expression signals (blue color) were located in the stromal cells at all ages (denoted by asterisks). AIB1 expression was not detected in the epithelium at 12 weeks (arrows), but detected in some of the transformed epithelial cells in the PIN region at 18 weeks. Further elevated AIB1 expression was seen in most of the epithelial or tumor cells in MDA and PDA at 24 and 30 weeks. Arrows indicate epithelial cells. LE, luminal epithelial cells; L, lumen.

D. *In situ* hybridization. *In situ* hybridization was performed with AIB1 antisense and sense riboprobes on prostate cryosections prepared from 12-, 18-, 24- and 30-week old WT/TRAMP mice. AIB1 mRNA signals (brown to purple color) were specifically detected by the antisense probe but not the negative control sense probe and these signals were increased in MDA and PDA at 24 and 30 weeks.

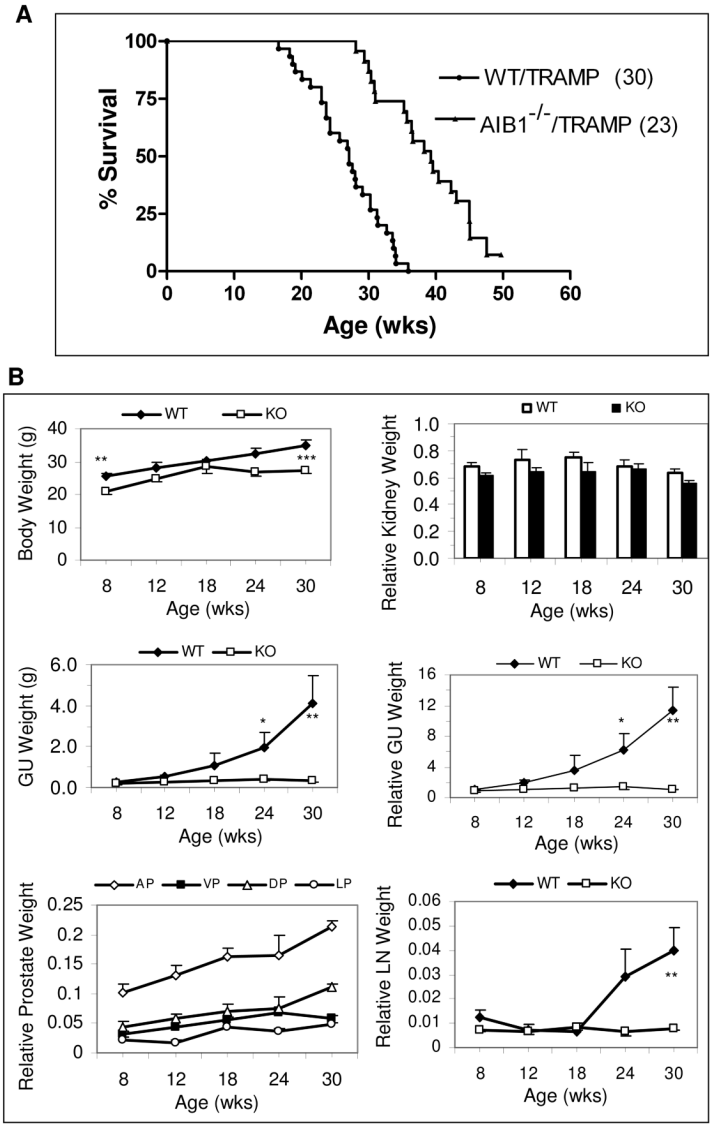

Fig. 3. Loss of AIB1 increases survival rate and reduces prostate tumor burden

A. Survival curves of WT/TRAMP and AIB1$^{-/-}$/TRAMP mice. Percentage of survival is plotted against their ages. The survival rates are statistically different between WT/TRAMP (n = 30) and AIB1$^{-/-}$/TRAMP (n = 23) mice (P < 0.0001; Log-rank test).

B. Change of GU and prostate weights in WT/TRAMP (WT) and AIB1$^{-/-}$/TRAMP (KO) mice during prostate tumor progression. Body weight, relative kidney weight, GU weight, relative GU weight, relative weights of prostate lobes and relative weight of peri-aortic lymph nodes (LN) were recorded as a function of ages. Relative weight was calculated by (weight × 100)/ body weight. *, 0.05 < P < 0.1; **, 0.01 < P < 0.05; ***, 0.001 < P < 0.01 (unpaired *t* test, n = 6).

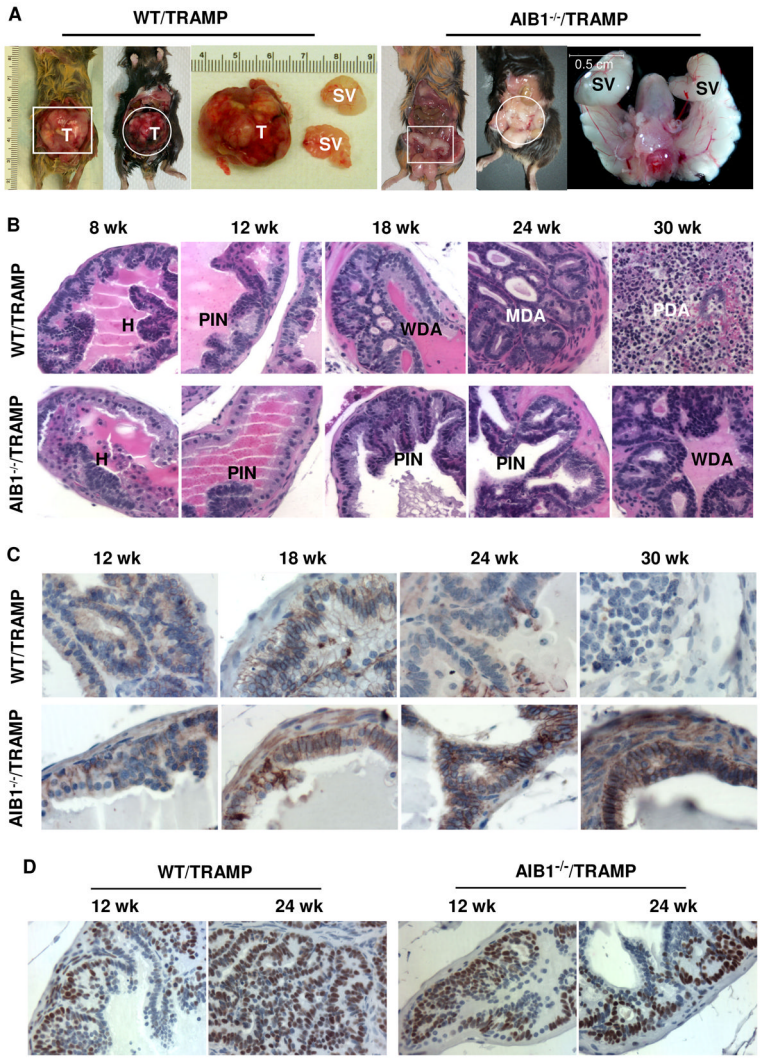

Fig. 4. Inactivation of AIB1 arrests prostate cancer progression and maintains E-cadherin expression without affecting the SV40 transgene expression

A. AIB1 deficiency inhibits prostate tumor formation. Necropsy was performed to examine the genitourinary (GU) tract of 30-week-old WT/TRAMP and AIB1$^{-/-}$/TRAMP mice. Panels 1 and 2 are representative photographs of typical prostate tumors in WT/TRAMP mice. The first tumor is also shown as an enlarged image. Panels 3 and 4 show apparently normal GU tracts in two AIB1$^{-/-}$/TRAMP mice. One of the GU tracts is also shown as an enlarged image. T, tumor; SV, seminal vesicle.

B. H&E-stained histological sections of the prostates prepared from WT/TRAMP and AIB1$^{-/-}$/TRAMP mice with indicated ages. Images were taken at 400X magnification. See text for differences of tumor progression in these mice. H, hyperplasia; PIN, prostate intraepithelial neoplasia; WDA, well-differentiated adenocarcinoma; MDA, moderately differentiated adenocarcinoma; PDA, poorly differentiated adenocarcinoma.

C. Immunohistochemical analysis of E-cadherin during prostate tumor progression in WT/TRAMP and AIB1$^{-/-}$/TRAMP mice. Sections from dorsal lobes were immunostained with an antibody against E-cadherin. Images were taken at 400X magnification. Brown color indicates E-cadherin immunoreactivity. Sections were counterstained with hematoxylin. Note that E-cadherin was detected in AIB1$^{-/-}$/TRAMP prostates at all ages, but in WT/TRAMP prostates E-cadherin was restricted in certain areas at 24 weeks and undetectable in PDA at 30 weeks.

D. IHC analysis of SV40 T antigen expression in WT/TRAMP and AIB1$^{-/-}$/TRAMP prostates and tumors. Sections from dorsal lobes were reacted with T antigen antibody. Images were taken at 400X magnification. Slides were counterstained with hematoxylin. Brown color reflects T antigen immunoreactivity. Note the T antigen immunoreactivities are similar in individual epithelial and tumor cells in both WT/TRAMP and AIB1$^{-/-}$/TRAMP mice, while the number of T antigen-positive cells increases significantly as prostate tumor progresses in WT/TRAMP mice.

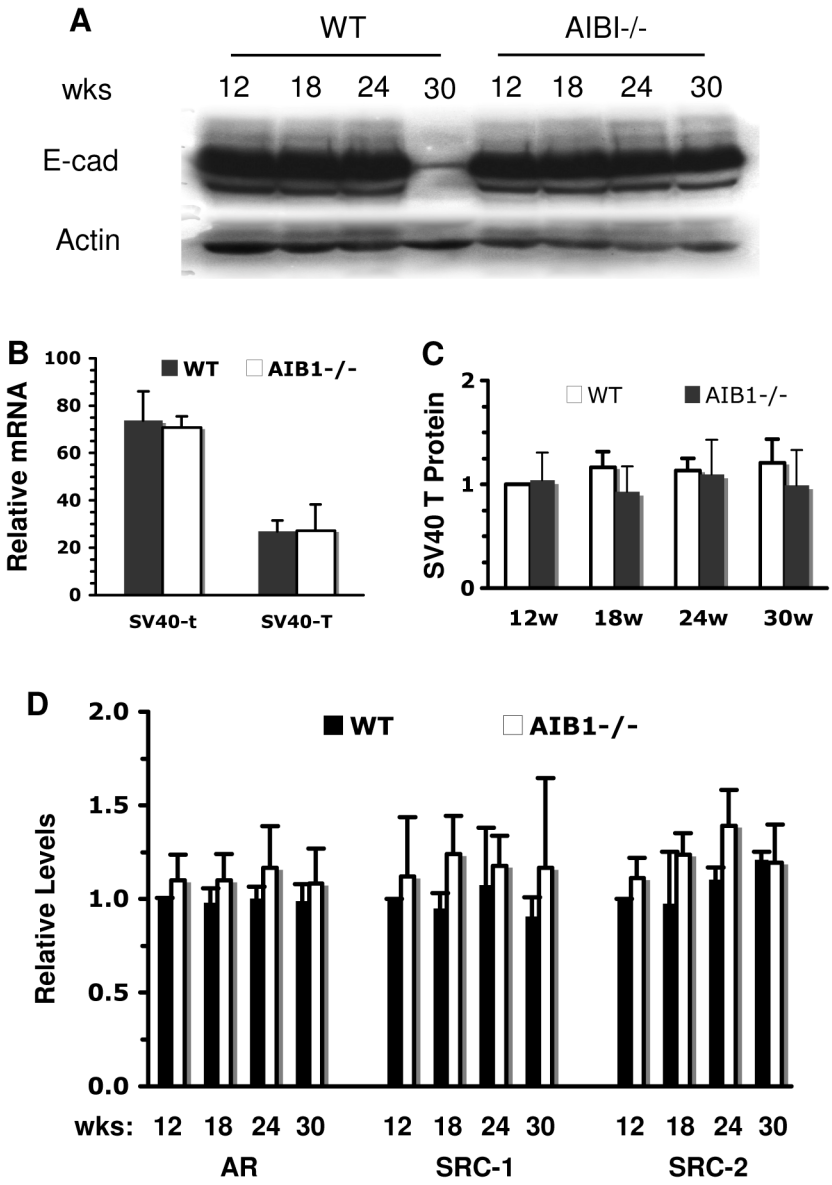

Fig. 5. Protein level analysis for E-cadherin, SV40 T, AR, SRC-1 and SRC-2

A. Western blot analysis of E-Cadherin in the prostates of WT/TRAMP (WT) and AIB1$^{-/-}$/TRAMP (AIB1−/−) mice. Note the striking reduction of E-Cadherin at 30 weeks when PDA developed in WT/TRAMP mice. β-actin was used as a loading control.

B. Real-time RT-PCR analysis of the PB-Tag transgene expression. Serial dilutions of a WT/TRAMP prostate RNA were used for generation of relative standard curve. 150 ng of RNA was used for each assay. The relative expression levels (arbitrary unit) of SV40 t and SV40 T mRNAs were normalized to the endogenous K18 mRNA levels. RNA samples prepared from three mice in each group were individually assayed with two repeats. Data are presented as mean SD. There are no statistical differences between WT/TRAMP and AIB1$^{-/-}$/TRAMP prostates in either SV40 t or T expression.

C. Western blot analysis of SV40 T antigen in the prostates. All prostate lobes or tumors were isolated from WT/TRAMP (WT) and AIB1$^{-/-}$/TRAMP (AIB1−/−)mice at indicated ages. Western blot was performed with antibodies against SV40 T antigen and CK8, an epithelial marker protein, by using 3 independent sets of samples. Band intensity was quantified by

densitometry. The relative T antigen levels were normalized to CK8 and the value for the 12-week WT/TRAMP prostate was set as 1. Data were presented as Mean ± SEM.

D. Western blot analysis of AR, SRC-1, and SRC-2 proteins in the prostates. Samples were prepared as described above from WT/TRAMP (WT) and AIB1$^{-/-}$/TRAMP (AIB1−/−) mice at indicated ages. Western blots were performed with antibodies specific to AR, SRC-1, SRC-2, and β-actin by using 3 independent sets of samples. Band intensity was quantified by densitometry. Relative protein levels were normalized to β-actin and the value for the 12-week WT/TRAMP prostate was set as 1. Data were presented as Mean ± SEM.

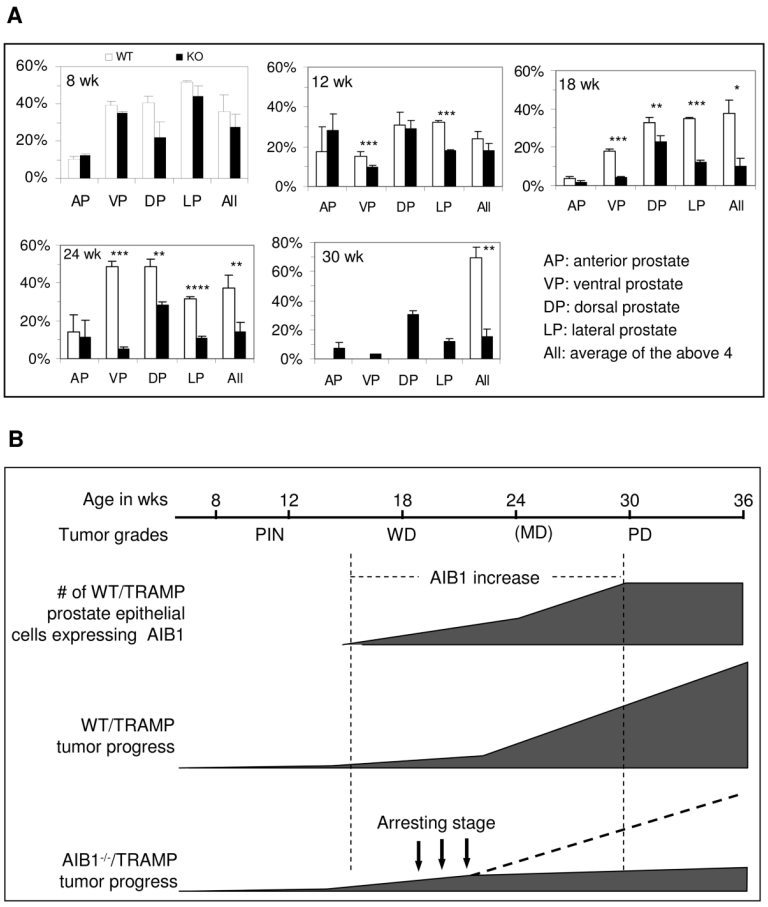

Fig. 6. Inactivation of AIB1 gene reduces cell proliferation

A. Analysis of cell proliferation by immunohistochemical staining of Ki67. The prostate lobes were isolated from WT/TRAMP (WT) and AIB1$^{-/-}$/TRAMP (AIB1−/−) mice with indicated ages. IHC was performed on de-paraffinized tissue sections by using Ki67 antibody. Images were recorded for quantitative analysis. The percentage of proliferating cells was determined by counting the Ki67-positive cells and total cells. For each age and genotype group, sections were prepared from AP, VP, DP and LP lobes of more than three animals, and at least 500 prostate cells were counted in more than three randomly selected areas on each section. *, 0.05 < P < 0.1; **, 0.01 < P < 0.05; ***, 0.001 < P < 0.01; ****, P < 0.0001 (unpaired *t* test).

B. Schematic relationships between AIB1 expression and prostate cancer progression. AIB1 expression appears in certain transformed epithelial cells between 12 and 18 weeks of age and further increases in and expands to a large population of transformed epithelial cells in WDA and MDA at 24 weeks of age, followed by a rapid tumor growth and malignant progression to PDA by 30 weeks in WT/TRAMP mice. Inactivation of AIB1 function arrests prostate tumor progression at WD carcinoma stage in AIB1$^{-/-}$/TRAMP mice, which is correlated with the timing of AIB1 induction before 24 weeks in WT/TRAMP mice.